Mon. Not. R. Astron. Soc. **000**, 1–10 (2008) Printed 20 August 2009 (MN LaTeX style file v2.2)

A survey for post common-envelope binary stars using GALEX and SDSS photometry ⋆

P.F.L. Maxted[1], B.T. Gänsicke[2], M.R. Burleigh[3], J. Southworth[2], T.R. Marsh[2], R. Napiwotzki[4], G. Nelemans[5], P.L. Wood[1]
[1] *Astrophysics Group, Keele University, Keele, Staffordshire ST5 5BG, United Kingdom*
[2] *Department of Physics, University of Warwick, Coventry CV4 7AL*
[3] *Department of Physics and Astronomy, University of Leicester, University Road, Leicester LE1 7RH*
[4] *Centre for Astrophysics Research, STRI, University of Hertfordshire, College Lane, Hatfield AL10 9AB*
[5] *Department of Astrophysics, IMAPP, Radboud University Nijmegen, PO Box 9010, 6500 GL Nijmegen, The Netherlands*

Submitted 2009

ABSTRACT

We report the first results of our programme to obtain multi-epoch radial velocity measurements of stars with a strong far-UV excess to identify post common-envelope binaries (PCEBs). The targets have been identified using optical photometry from SDSS DR4, ultraviolet photometry from GALEX GR2 and proper motion information from SDSS DR5. We have obtained spectra at two or more epochs for 36 targets. Three of our targets show large radial velocity shifts ($> 50\,\mathrm{km\,s^{-1}}$) on a timescale of hours or days and are almost certainly PCEBs. For one of these targets (SDSS J104234.77+644205.4) we have obtained further spectroscopy to confirm that this is a PCEB with an orbital period of 4.74 h and semi-amplitude $K = 165\,\mathrm{km\,s^{-1}}$. Two targets are rapidly rotating K-dwarfs which appear to show small radial velocity shifts and have strong Ca II H+K emission lines. These may be wind-induced rapidly rotating (WIRRing) stars. These results show that we can use GALEX and SDSS photometry to identify PCEBs that cannot be identified using SDSS photometry alone, and to identify new WIRRing stars. A more comprehensive survey of stars identified using the methods developed in this paper will lead to a much improved understanding of common envelope evolution.

Key words: binaries: spectroscopic – ultraviolet: stars – white dwarfs – stars: late-type

1 INTRODUCTION

Post common-envelope binary stars (PCEBs) can be loosely defined as short period binary stars containing a compact object. Cataclysmic variable stars (CVs), in which a white dwarf accretes matter from a low-mass star that fills it Roche lobe, are one example of PCEBs. Compact objects are generally the result of stellar evolution involving at least one phase when the star is a red giant, but the size of a giant star exceeds the current separation of the stars in a PCEB by a few orders of magnitude. Paczynski (1976) outlined the solution to this puzzle in a short paper on the origins of CVs that describes the main features of what is commonly known as common envelope evolution. In the case of CVs, the evolution begins with a star of a few solar masses with a less massive companion in a wide orbit. The evolution of the more massive star through the red giant phase is terminated prematurely when it exceeds the size of its Roche lobe. The resulting mass transfer onto the low-mass companion is dynamically unstable, so the companion is unable to accrete the material from the red giant. The material forms a common envelope around the dense core of the red giant and the low-mass companion. If the companion is not massive enough to force the envelope to co-rotate then the evolution proceeds on a dynamical timescale as dynamical friction forces the low-mass companion to spiral in through the outer layers of the red giant. The orbital energy lost by the companion is transfered to the outer layers of the red giant, which are ejected to reveal the hot, degenerate core of the red giant and, if it survives, the low-mass companion. Angular momentum loss by a combination of a magnetic stellar wind and gravitational wave radiation, or the evolution of the companion may lead to a second phase of Roche lobe overflow, this time from the low-mass companion onto the white dwarf, i.e., the formation of a CV. For this reason, detached binary stars containing a low mass star and white dwarf with an orbital period of about a day or less are known as pre-CVs (Schreiber & Gänsicke 2003).

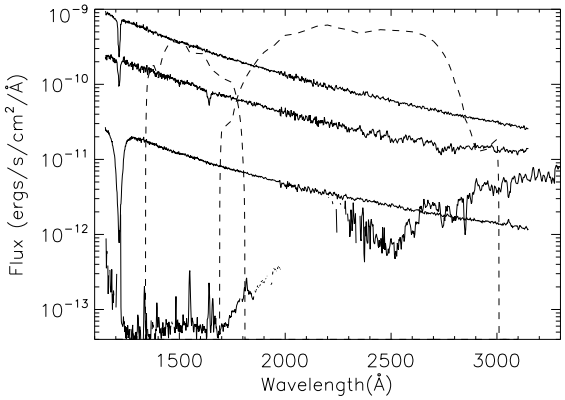

Figure 1. The GALEX FUV and NUV response (arbitrary units) compared to IUE spectra of 3 white dwarfs (HD 149499 B DOZ1; G191-B2B, DA1 and EG 274, DA2), and an active solar-type star EK Dra (in order of decreasing FUV flux). All fluxes scaled to a distance of 10 pc.

The compact object in a PCEB may be a neutron star (NS), black hole (BH) or white dwarf (WD). Short period binary stars containing hot subdwarf stars (sdO or sdB stars) are also considered to be PCEBs. The companion star in a PCEB may be a non-degenerate star or another compact object, e.g., binary pulsars (NS+NS), ultra-compact X-ray binaries (WD+NS) or AM CVn binaries (WD+WD).

There is a vast literature on the theory of the common envelope phase and many published models of the population of PCEBs (Postnov & Yungelson 2006; Iben & Livio 1993; Taam & Sandquist 2000). Considerable debate continues over fundamental aspects of the CE phase, much of it focused on the definition and value of the parameter $\alpha_{\rm CE} = \frac{E_{\rm env}}{\Delta E_{\rm orb}}$, where $\Delta E_{\rm orb}$ is the change in orbital energy of the binary during the CE phase and $E_{\rm env}$ is the change in the binding energy of the red giant envelope. In theory, the outcome of the CE phase for a given binary can be calculated given a known value for the parameter $\alpha_{\rm CE}$. In practice, it is unclear whether the definition of $E_{\rm env}$ should include energy sources other than the gravitational potential energy of the envelope (Soker & Harpaz 2003; Dewi & Tauris 2000; Han et al. 2002; Beer et al. 2007; Webbink 2008), whether evolution prior to Roche lobe overflow is important (Eggleton 2002; Soker 2004) or whether a balance of energies gives a valid description of the CE phase (Nelemans et al. 2000; Nelemans & Tout 2005). These debates are driven by the discovery and characterization of PCEBs whose properties, either individually or as a group, are not easily explained by a simple model of the CE phase, e.g., detached WD+WD "double degenerate" binaries (Maxted et al. 2002a,b) and sdB stars (Maxted et al. 2004). Davis et al. (2009) have recently compared the results of binary population synthesis models for a range of input parameters and using different parametrizations of the common envelope phase to the observed properties of 35 PCEBs. They find that the standard $\alpha_{\rm CE}$ parametrization can account for the observed properties of PCEBs with late-type companions to (pre-)white dwarfs, but cannot explain IK Peg which has an A8 companion star. They conclude that "the detection of more PCEBs with early type secondaries may shed further light on the CE phase". They also find that there is a sharp decline in the observed number of PCEBs with periods > 1 day that cannot be reproduced by any of the models considered, even if the selection biases against longer period systems are accounted for. This suggests there are some important features of the common envelope phase that are not included in the current models.

One way to better understand the common envelope (CE) phase is to compare the predictions of binary population synthesis models to the properties of a large, homogeneously selected sample of PCEBs for which the selection effects are well understood. This has the advantage of giving a result that is valid for the general population of that type of PCEB. Comparison of models to one or two systems may lead to spurious conclusions if one of the systems has had a peculiar history, e.g., V471 Tau appears to be a normal PCEB containing a white dwarf and a K-dwarf, but its membership of the Hyades enables us to infer that it has a peculiar evolutionary history and is probably the result of the evolution of a triple star system (O'Brien et al. 2001).

The Sloan Digital Sky Survey (SDSS) makes it possible to construct a well-defined sample of PCEBs that can be identified from their optical colours. This is particularly so for non-interacting binaries containing a WD with M-dwarf companions (WD+M). These binaries have distinctive colours that enable them to be efficiently identified from the SDSS photometry alone, (Augusteijn et al. 2008; Schreiber et al. 2007; Yanny 2009) and there is also spectroscopy of many such systems from the same survey (Heller et al. 2008; Rebassa-Mansergas et al. 2007). There are also many CVs with SDSS spectra that have been targeted for observation from their SDSS colours or observed serendipitously (Szkody et al. 2007). The selection effects for CVs are large and depend strongly on their accretion properties, whose dependence on the other properties of the binary are themselves poorly understood. For this reason, detached PCEBs are a better choice than CVs as a sample for testing models of CE evolution for WD binaries.

Using SDSS photometry alone it is only possible to detect unresolved non-interacting binaries if the companion to the white dwarf has a spectral type later than about M0, the exact limit depending on the temperature of the white dwarf (Augusteijn et al. 2008). Schreiber & Gänsicke (2003) calculated the temperature of the coolest WD that can be detected from a U-band excess as function of spectral type for a main-sequence companion. The limits are approximately 45,000K, 28,000K and 9,000K for spectral types K5, M0 and M6, respectively. The limits will be similar for the SDSS or any survey based on optical photometry because for cooler WDs the main-sequence companion is much brighter than a non-accreting WD at all optical wavelengths.

To find non-accreting white dwarfs with F-, G- and K-type companions or to find cool WDs with M-type companions requires a survey at UV or soft X-ray wavelengths. Landsman et al. (1996) identified two late-type stars with hidden hot white dwarfs (56 Per and HR 3643) from follow-up observations of late-type stars with a 1565Å excess in the TD-1 ultraviolet sky survey. These are Sirius-like binaries, i.e., non-interacting systems with large orbital separations. Many more Sirius-like binaries were identified as a result of the EUVE and ROSAT surveys (Burleigh 2002). These surveys also identified several new PCEBs (Burleigh et al. 1997;

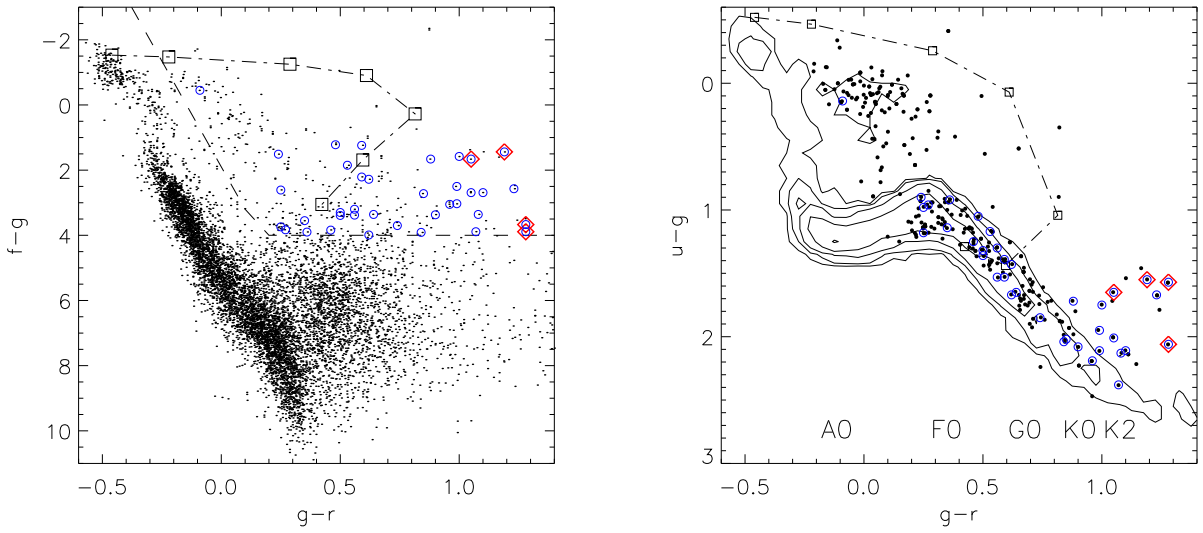

Figure 2. Colour-colour diagrams for our sample of stars with reliable optical and ultraviolet photometry. The limit for selecting stars with an ultraviolet excess is shown in the left panel as a dashed line. Stars above this line are plotted with dots in the right panel. For clarity, we show the density of points in the right panel with contours rather than individual points. An approximate indication of spectral type for single stars based on their $g-r$ colour is indicated in the bottom of the right panel. Stars for which we have obtained spectra are circled and stars with variable radial velocities are marked with diamonds. The dash-dot line with squares shows the combined colours of a white dwarf with $T_{\rm eff}$ =48,000K plus cool companions with spectral types from G2 to M5 (the blue-most point is the white dwarf alone).

Barstow et al. 1994; Vennes et al. 1998). There have also been serendipitous discoveries, e.g., from IUE spectroscopy (Böehm-Vitense 1993, 1992). These serendipitous discoveries can provide useful evidence for the existence of a particular type of binary star, but it is difficult to know whether they should be included in any test of a binary population synthesis model.

The advent of the GALEX all-sky UV survey (Martin et al. 2005) makes it feasible to conduct a large survey to detect hot white dwarfs in unresolved binaries with G-type and K-type companions and cool WD with early-M type companions. In this paper we report the first results of our survey to obtain follow-up spectroscopy of solar-type stars with a far-UV excess identified using GALEX and SDSS photometry. The main aim of the survey is to produce a well-defined sample of detached PCEBs that cannot be identified using SDSS photometry alone. The properties of these PCEBs will be a strong test of population synthesis models. We also expect that this survey will find other interesting objects, e.g., CVs and other interacting binary stars.

2 TARGET SELECTION

To discover PCEBs in which the non-degenerate companion dominates the optical flux we require a sample of stars with reliable optical and ultraviolet photometry. We also require that the sources are bright so that the follow-up of the targets can be done efficiently. To produce this sample of stars we used optical SDSS photometry and ultraviolet GALEX photometry. We started with the table provided by Multimission Archive at STScI of objects from SDSS DR4 cross matched within 4 arcsec of objects in GALEX GR2 (table xSdssDr4). From this table we selected objects satisfying the following criteria:

- $< 0.6^\circ$ from the centre of the GALEX field of view;
- the closest SDSS object to the GALEX source position;
- GALEX magnitudes $n < 25$ and $f < 25$;
- SDSS g-magnitude $g < 16.5$;
- SDSS morphological type class 6 (STAR);
- "clean" SDSS photometry;[1]
- proper motion > 0.01 arcsec/yr.

The g magnitudes used in this paper are taken from the SDSS table entry psfMag_g, and similarly for other SDSS magnitudes. The resulting table has 2960 sources. Although the matching radius is 4 arcsec, the positions for GR2 and DR4 agree to within 1 arcsec for 80% of the sources. The restriction on the source position in the field of view is to avoid spurious detections that are common in these regions (Agüeros et al. 2005). The proper motion information was taken from a table provided by SDSS DR5 and is based on the astrometry from the SDSS plus recalibrated USNO-B astrometry. Objects detected at fewer than 6 epochs in SDSS plus USNO-B were excluded. This restriction on the proper motion was included to reduce the contamination of the sample by background sources (galaxies and quasars). Without this criterion the sample size would be 8760 sources. The disadvantage of adding this proper motion criterion is that it introduces a kinematical bias into the survey. A complete treatment of this bias is beyond the scope of this paper.

[1] *See http://skyserver.sdss.org/dr2/en/help/docs/ realquery.asp#flags*

The majority of objects in this sample of 2960 sources are expected to be moderately bright stars with reliable optical and ultraviolet photometry. There are no stars brighter than $g = 13$ in the sample because stars brighter than this appear saturated in the SDSS images so they do not have reliable SDSS photometry.

The far-UV (FUV) and near-UV (NUV) passbands of the GALEX instrument are shown in Fig. 1 and are compared to the UV spectra of three WDs and a very active G0V star. It can be seen that hot WDs (DA2 or hotter) can be easily distinguished from an active solar-type stars at FUV wavelengths.

NUV and u-band fluxes can be strongly affected by chromospheric activity in late-type stars (Fig. 1), so we used the $f-g$ colour to identify stars with a UV excess. The distribution of these sources in the $f-g$ v. $g-r$ and $u-g$ v. $g-r$ colour-colour diagrams are shown in Fig. 2. There is a well defined main-sequence relation in the optical colour-colour diagram, showing that the optical photometry for the majority of stars in our sample is reliable. Our criteria for selecting stars with a UV excess as shown in this figure are

$$(f-g) < 13(g-r) + 1.9 \quad \text{and} \quad (f-g) < 4.$$

There are 90 targets that satisfy these selection criteria.

2.1 Cross-identifications for target objects

We have used the SIMBAD database to search for catalogued objects matching our target positions. The results are given in Table 1 and some individual objects are discussed below. These stars give some impression of the type of object that may be discovered using our survey. In most cases, but not all (e.g. U Sex), we avoided observing objects where the nature of the star was already clear from existing observations.

KUV 03134−0001 The spectral type of this star given by Wegner & Dupuis (1993) is "cont. + dM – Composite spectrum; shows blue continuum plus TiO features in the red".

PQ Gem A well-known intermediate polar (Evans et al. 2006; Rosen et al. 1993).

J0852+0313 The SDSS spectrum of this object shows that it is a QSO with a redshift $z = 0.297$. There is a faint companion within a few arcseconds to this QSO visible in the SDSS images that is unresolved in the DSS images from which the USNO-B positions are measured. We conclude that the proper motion value for this object is spurious.

BZ UMa This is a dwarf nova (CV, Neustroev et al. 2006).

PG 1056+324 Wagner et al. (1988) give a spectral type of "sdB" for this star.

BE UMa This is a well-studied detached PCEB containing a very hot (pre-)white dwarf and a low-mass, non-degenerate companion with an orbital period of 2.3 d (Ferguson et al. 1999).

SDSS J140916.11+382832.1 The automatic classification algorithm of Eisenstein et al. (2006) identifies this star as a hot subdwarf. Visual inspection of the SDSS spectrum shows hints of absorption lines due to a late-type companion (G-band, Mg-b, Ca II IR triplet).

SBSS 1422+497 The spectral type given by Stepanian (2005) is "DA".

PG1657+416 This is a pulsating sdB star with a G5 main-sequence companion star (Oreiro et al. 2007).

2.2 Observations

We obtained spectroscopy for 36 targets from our sample using the Intermediate Dispersion Spectrograph (IDS) on the 2.5m Isaac Newton Telescope. We used the H2400B grating with a 1.2 arcsec slit and the EEV10 charge coupled device (CCD) detector to obtain spectra with a resolution of 0.45Å sampled at 0.22Å/pixel. The unvignetted portion of the CCD covers the wavelength range 4875 – 5375Å. We also extracted the region of the spectrum around the Hβ line that lies in the vignetted region of the CCD. Spectra were extracted using the optimal extraction algorithm of Horne (1986). Observations of each star were bracketed with arc spectra and the wavelength calibration established from these arcs interpolated to the time of mid-exposure. We obtained a single spectrum of 19 of our targets on 2007 Jan 29. The majority of the spectra were obtained in the interval 2008 Dec 20 to 2008 Dec 26. The average spectrum of each target is shown in Fig. 3.

We measured the radial velocity (RV) of our targets using cross correlation against a spectrum of the RV standard star HD 65583 (G8V, $V_r = +14.85\,\mathrm{km\,s^{-1}}$; Udry et al. 1999). The spectral range used for the cross-correlation was 4868 – 5395Å. We obtained spectra of the RV standard star HD 3765 on every night of the 2007 Jan and 2008 Dec runs to monitor the stability of our RV measurements. The standard deviation of the RV measurements from these spectra is $2.79\,\mathrm{km\,s^{-1}}$. This is much larger than the precision with which the peak of the cross-correlation function (CCF) can be located and is likely to be dominated by the motion of the stellar image within the spectrograph slit. We added this estimate of the external error in quadrature to the internal error of the RV measurements of our targets to obtain a total standard error estimate for each RV measurement. The exposure times used for our targets (300 – 1800s) are much longer than those used for HD 3765 (30 – 60s). Guiding errors during a longer exposure will smear the light of the star across the slit so the external error due to image motion in the slit is likely to be less for our targets than for HD 3765, i.e., the total standard errors we have adopted are likely to be pessimistic.

For the set of RV measurements of each target $V_{r,i}$; $i = 1, \ldots, N_{\mathrm{RV}}$, we calculate the weighted mean RV value, $\overline{V}_r$. To test for variability of the RV we calculate the probability, p, of obtaining the observed value of χ^2 or greater for the model $V_{r,i} = \overline{V}_r$ assuming normally distributed errors, i.e., a small value of p indicates that the RV measurements are not constant. The value of p for each target are also given in Table 2 as $\log p$.

Also shown in Table 2 is a crude estimate of the equivalent width of the Hβ line, EW(Hβ) in the average (median) spectrum of the star after shifting the individual spectra to a common wavelength scale according to their measured RVs. The equivalent width was calculated by numerical integration in a window ±5Å wide around the rest wavelength of the line. Negative values of EW(Hβ) indicate that the Hβ line is in emission.

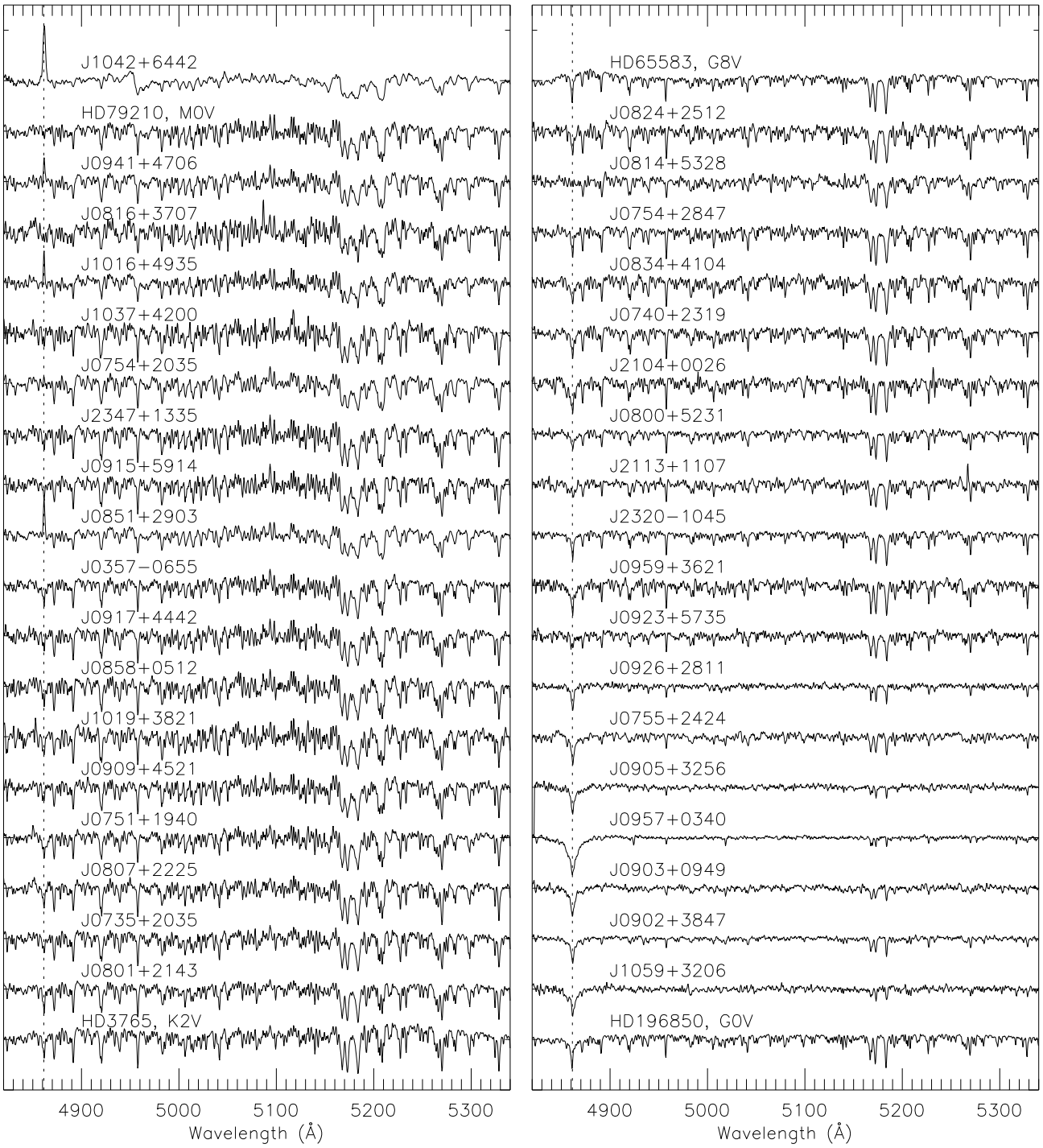

Figure 3. Spectra of our targets ordered by their $g-r$ colour. Spectra have been co-added on a common wavelength scale, normalized, smoothed and re-binned for display and are offset by 1 for clarity. Spectra of some radial velocity standard stars with known spectral types as shown in the label are included for comparison. The rest wavelength of the Hβ line is indicated with a dotted line.

3 RESULTS

3.1 Detection efficiency

For each star we calculate the probability of detecting a companion from the radial velocity variations using the method of Maxted et al. (2001). We assume a mass of $0.75M_{\odot}$ for the visible star because this is likely to be close to the average mass of our target stars. We assume a mass ratio of $q = 0.75$ because this value then gives a white dwarf companion mass of $0.56M_{\odot}$, which is a typical mass for a white dwarf. The results for two stars are shown in Fig. 4. We find that the average detection efficiency near a period of 10 d is

Table 1. Cross-identifications for objects from our sample with sources listed by SIMBAD.

ID	α_{2000}	δ_{2000}	g	$u-g$	$g-r$	$f-g$	Other ID	Notes
J0316+0009	03 16 00.2	+00 09 47	16.45	0.52	0.65	0.06	KUV 03134-0001	
J0751+1444	07 51 17.3	+14 44 24	14.18	−0.06	0.18	1.44	PQ Gem	Intermediate polar
J0824+3028	08 24 34.1	+30 28 55	15.25	0.09	−0.07	−0.44	PG 0821+306	QSO
J0852+0313	08 52 59.2	+03 13 21	16.22	0.08	0.06	1.30	2MASS J08525922+0313207	
J0853+5748	08 53 44.2	+57 48 41	16.40	−0.41	0.35	0.74	BZ UMa	Dwarf nova
J0941+4706	09 41 55.2	+47 06 38	16.12	2.06	1.28	3.89	XMS J094154.6+470637	
J0957+0340	09 57 25.4	+03 40 05	14.91	1.18	0.25	2.61	U Sex	RR Lyrae star
J1014+0033	10 14 54.9	+00 33 37	16.27	0.08	0.16	0.66	QSO B1012+008	
J1042+6442	10 42 34.8	+64 42 05	15.00	1.57	1.28	3.67	1RXS J104237.0+644217	
J1054+3600	10 54 50.6	+36 00 13	16.48	2.47	0.96	3.12	LEDA 3088408	
J1059+3206	10 59 05.2	+32 06 21	14.64	0.14	−0.09	−0.45	PG 1056+324	sdB
J1121+0012	11 21 19.7	+00 12 12	14.90	1.18	0.42	3.38	2MASS J11211965+0012120	
J1155+0640	11 55 28.1	+06 40 18	15.70	1.05	0.43	1.91	Pul−3 850246	
J1157+4856	11 57 44.8	+48 56 18	15.78	−0.28	−0.10	−1.72	BE UMa	PCEB, P=2.3 d
J1300+4139	13 00 40.1	+41 39 37	15.07	0.94	0.34	3.05	BPS BS 16938-0017	
J1409+3828	14 09 16.1	+38 28 32	16.03	−0.13	−0.16	−1.03	SDSS J140916.11+382832.1	
J1418+3705	14 18 31.8	+37 05 41	15.41	1.27	0.46	2.99	2MASS J14183182+3705411	
J1424+4929	14 24 40.5	+49 29 58	16.24	0.10	0.49	−1.06	SBSS 1422+497	DA
J1658+4131	16 58 41.8	+41 31 16	15.93	−0.09	−0.21	−0.86	PG 1657+416	sdB+G5V

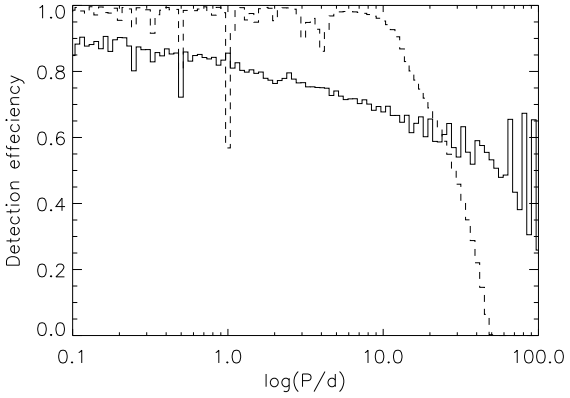

Figure 4. The fraction of binaries detected with $\log p < -3$ assuming a mass ratio $q = 0.75$ and a mass for the visible star of $0.75 M_{\odot}$ using data with the same sampling and standard errors as that obtained for J0801+2143 (solid line) and J0909+4521 (dashed line). The detection efficiency in each bin is the average of 100 periods evenly distributed between the bin limits.

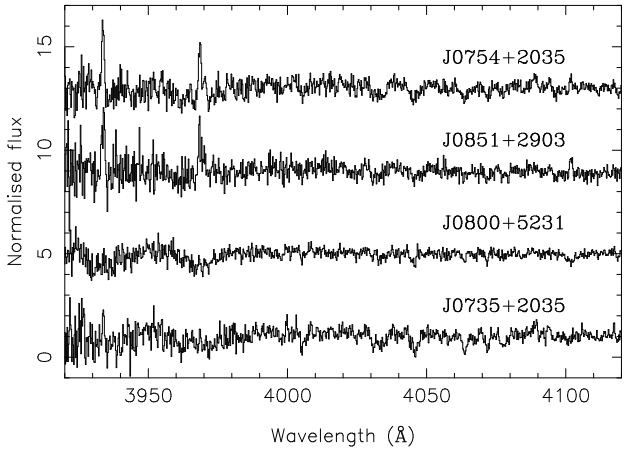

Figure 5. Spectra of selected targets in the region of the Ca II H and K lines. The spectra have been normalized, smoothed and vertically offset for clarity.

79% and that the detection efficiency is more than 50% for periods of less than 10 d for all 36 of the stars observed.

3.2 Notes on individual objects

J0754+2035 We obtained a single spectrum of this star with the IDS and the H2400B grating at a central wavelength of 4200Å. This spectrum shows strong emission in the cores of the Ca II H and K lines (EW ≈ -3.5Å) for this star (Fig. 5). The width of the CCF in this star shows this star is a rapid rotator and so is expected to be chromospherically active. There is some weak evidence for a small amount of RV variability in this star ($\approx 10 \mathrm{km\,s^{-1}}$), which may be a result of star spots rather than binarity.

J0800+5231 There is an offset of about $10 \mathrm{km\,s^{-1}}$ between the RVs measured for this star in 2007 and 2008, but no significant variability over 4 nights from the 2008 data alone. This may be a binary with a long orbital period. A single spectrum near 4200Å obtained with the IDS (Fig. 5) suggests that the spectral type is late-G, which is consistent with the $u-g$ and $g-r$ colours of the star.

J0814+5328 The spectra near the Hβ line are noisy but the absorption line does appear to be shallow compared to other stars of the same colour/spectral-type (Fig. 3). The absorption line may be "filled-in" by weak emission at this wavelength.

J0851+2903 This is a similar case to J0754+2035. A single spectrum around 4200Å shows Ca II H and K lines in emission (EW ≈ -3Å, Fig. 5), and there is some evidence of RV variability at the level of $20 \mathrm{km\,s^{-1}}$ which may be the result of star spots in this rapidly rotating star.

J0905+3256 This star has a large heliocentric RV ($\approx -320 \mathrm{km\,s^{-1}}$) so is likely to be a halo star.

J0941+4706 This star is an X-ray source detected by the XMS survey (Barcons et al. 2007). The RV changes by more

Table 2. Summary of our radial velocity measurements. N_{rv} is the number of radial velocity measurements. Δt is the baseline of the observations. See text for the definition of $\log p$. FWHM is the mean full-width at half-maximum of the CCF. Where a $\star$ symbol appears in the final column further remarks on the star appear in Section 3.2.

ID	RA (J2000)	Dec (J2000)	g	$u-g$	$g-r$	$f-g$	N_{rv}	$\log p$	Δt (days)	EW(Hβ) (Å)	FWHM ($\mathrm{km\,s^{-1}}$)	
J0357−0655	03:57:16.0	−06:55:04	16.07	1.75	1.00	1.58	5	−0.10	693.1	1.4	70	
J0735+2035	07:35:34.5	+20:35:32	15.87	2.04	0.84	3.91	5	−0.51	696.1	0.7	67	
J0740+2319	07:40:33.6	+23:19:26	14.56	1.53	0.59	2.21	2	−0.02	691.1	1.8	65	
J0751+1940	07:51:32.0	+19:40:55	16.46	1.72	0.88	1.66	4	0.00	691.2	1.5	69	
J0754+2035	07:54:07.5	+20:35:52	16.12	2.13	1.08	3.36	6	−1.12	696.1	−0.4	113	$\star$
J0754+2847	07:54:04.2	+28:47:01	16.10	1.67	0.62	3.99	2	−0.25	691.2	1.4	67	
J0755+2424	07:55:41.9	+24:24:36	16.27	1.14	0.35	3.55	2	−0.35	692.1	2.4	86	
J0800+5231	08:00:38.6	+52:31:29	16.28	1.30	0.56	3.20	4	−2.69	696.0	1.1	69	$\star$
J0801+2143	08:01:07.1	+21:43:37	15.09	1.85	0.74	3.70	2	−0.17	691.2	1.2	69	
J0807+2225	08:07:36.5	+22:25:37	16.21	2.02	0.85	2.72	2	−0.03	691.2	1.0	73	
J0814+5328	08:14:43.4	+53:28:05	16.48	1.43	0.62	2.28	2	−0.23	692.0	0.1	92	$\star$
J0816+3707	08:16:07.1	+37:07:04	16.39	1.67	1.23	2.57	2	−0.11	691.1	0.9	69	
J0824+2512	08:24:56.5	+25:12:47	15.83	1.65	0.64	3.36	2	−0.25	691.2	1.7	67	
J0834+4104	08:34:50.0	+41:04:23	15.73	1.39	0.59	1.24	2	−0.14	691.2	1.5	65	
J0851+2903	08:51:37.2	+29:03:30	16.24	1.65	1.05	1.66	9	−2.16	696.1	−1.3	120	
J0858+0512	08:58:03.2	+05:12:49	15.84	2.11	0.99	3.03	2	−0.11	691.3	1.1	69	
J0902+3847	09:02:04.1	+38:47:38	14.74	0.90	0.24	1.51	6	−0.99	693.2	2.1	76	
J0903+0949	09:03:51.2	+09:49:35	16.38	0.98	0.25	3.74	3	−0.09	4.1	2.7	121	
J0905+3256	09:05:24.4	+32:56:02	15.24	0.96	0.27	3.83	4	−0.37	4.0	2.1	76	$\star$
J0909+4521	09:09:38.0	+45:21:42	15.63	2.08	0.90	3.37	3	−0.21	4.1	0.5	71	
J0915+5914	09:15:42.7	+59:14:57	15.84	2.01	1.05	2.69	3	−0.09	4.0	0.7	74	
J0917+4442	09:17:10.3	+44:42:26	15.84	1.95	0.99	2.50	4	−0.07	4.0	0.6	69	
J0923+5735	09:23:23.1	+57:35:40	15.25	1.05	0.48	1.22	3	−0.12	4.1	0.4	60	
J0926+2811	09:26:16.6	+28:11:13	15.98	0.92	0.36	3.90	4	−0.03	4.1	1.6	61	
J0941+4706	09:41:54.6	+47:06:38	16.12	2.06	1.28	3.89	4	< -40	4.0	−1.5	96	$\star$
J0957+0340	09:57:25.4	+03:40:05	14.91	1.18	0.25	2.61	3	−0.36	1.1	4.3	76	
J0959+3621	09:59:02.4	+36:21:03	14.49	1.36	0.50	3.39	2	−0.07	1.0	2.3	58	
J1016+4935	10:16:57.1	+49:35:14	16.11	1.55	1.19	1.44	4	< -40	3.9	−0.8	71	$\star$
J1019+3821	10:19:37.4	+38:21:12	15.41	2.19	0.96	3.05	2	−0.46	1.0	0.9	68	
J1037+4200	10:37:08.3	+42:00:39	15.78	2.11	1.10	2.69	2	−0.07	1.0	0.3	69	
J1042+6442	10:42:34.8	+64:42:05	15.00	1.57	1.28	3.67	9	< -40	3.0	−5.1	180	$\star$
J1059+3206	10:59:05.2	+32:06:21	14.64	0.14	−0.09	−0.45	2	−1.06	2.9	2.5	66	
J2104+0026	21:04:01.4	+00:26:54	16.29	1.53	0.56	3.38	2	−0.05	4.0	2.7	57	
J2113+1107	21:13:16.2	+11:07:48	16.31	1.17	0.53	1.85	2	−0.24	4.0	1.5	70	
J2320−1045	23:20:40.4	−10:45:11	15.22	1.32	0.50	3.30	6	−0.02	5.0	1.6	63	
J2347+1335	23:47:42.4	+13:35:57	15.54	2.38	1.07	3.89	4	−0.01	5.0	0.6	69	

than $50\mathrm{km\,s^{-1}}$ in less than 3 hours. This is too large to be explained by star spots. The Hβ emission line has a similar width to the CCF and shows the same RV variation, i.e., the Hβ emission is due to irradiation of and/or chromospheric activity on the M-dwarf and is not due to an accretion disc. This is almost certainly a PCEB.

J0957+0340 This is an RR Lyr-type variable star of type RRab (Kukarkin et al. 1971). The amplitude of the variability of these stars at UV wavelengths is very large (Wheatley et al. 2005), so it is not surprising that optical and UV photometry obtained at different epochs result in a peculiar position for the star in the UV-optical colour-colour diagram.

J1016+4935 The RV of this star changes by $\approx 100\mathrm{km\,s^{-1}}$ over 3 d. The Hβ emission line has a similar width to the CCF and shows the same RV variation, i.e., the Hβ emission is due to irradiation of and/or chromospheric activity on the M-dwarf. This is almost certainly a PCEB. We have too few data to estimate the orbital period.

J1042+6442 This star is an X-ray source detected by the ROSAT-FSC survey (Mickaelian et al. 2006). The RV changes by approximately $250\mathrm{km\,s^{-1}}$ in less than 3 hours. Additional spectroscopy has been obtained and is discussed in the next section.

3.3 J1042+6442

The data for this star obtained during 2008 Dec clearly show that the RVs vary with a period ~ 0.2 d. We obtained further spectroscopy with the same instrument and configuration during Jan 2009 to measure the orbital period and mass function of this star. A further 17 spectra were obtained, although some of these have poor signal-to-noise due to poor seeing. The RV of J1042+6442 was measured as above for all the spectra and are given in Table 3. We then searched for periodicity in these RV measurements by fitting sine waves at a range of trial frequencies. The period is found to be close to 0.19767 d and is unambiguous (Fig. 6). Also given

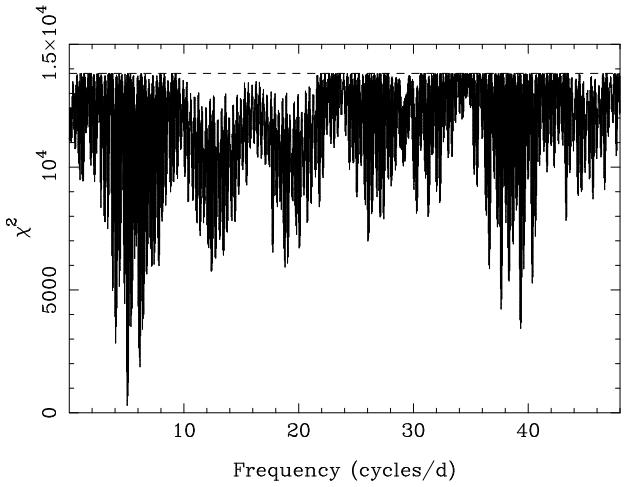

Figure 6. Periodogram of our RV measurements for J1042+6442. The value of χ^2 is shown for a least-squares fit of a sine wave at each frequency.

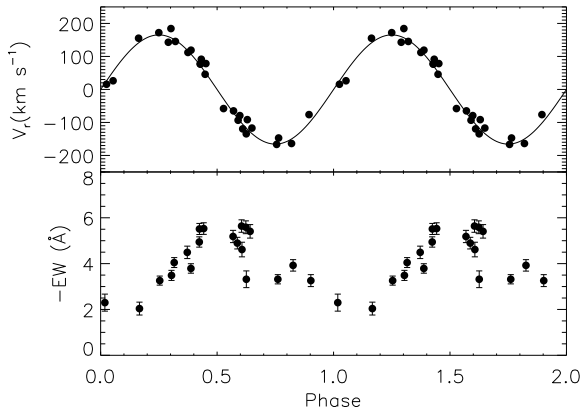

Figure 7. *Upper panel:* RV measurements of J1042+6442 with the circular orbit fit by least-squares plotted as a function of orbital phase for $P = 0.19767$ d. *Lower panel:* Equivalent width of the Hβ emission line. . Measurements with large uncertainties have been excluded for clarity.

in Table 3 is the equivalent width of the Hβ emission line measured by numerical integration in a window $\pm 250 \mathrm{km\,s^{-1}}$ around the position of the line based on the measured RV. We used a least-squares fit of a circular orbit to the RV measurements to derive the parameters shown in Table 4. The scatter of the RV measurements around the best fit is larger than expected given the standard errors of the RV measurements. We account for this by adding a quantity $\sigma_{\rm ex}$ in quadrature to the standard errors of the RV measurements prior to calculating the fit. The physical origin of $\sigma_{\rm ex}$ may be related to the extreme chromospheric activity that is expected for such a rapidly rotating M-dwarf. The RV measurements, circular orbit fit and EW(Hβ) measurements are shown in Fig. 7. The Hβ emission line has a similar width to the CCF and shows the same RV variation so it originates from the M-dwarf. There is a clear cosine-like variation of EW(Hβ) with orbital phase, as expected if it is due to the irradiation of one side of the M-dwarf by a hot companion. We applied a rotational broadening function to the spectra of HD 79210 (M0V) for various values of the projected equatorial rotational velocity, $\mathrm{V_{rot}} \sin i$ where i is the inclination, and measured the FWHM of the resulting CCF. From this calibration we estimate that the FWHM of $180 \mathrm{km\,s^{-1}}$ observed for the CCF of J1042+6442 corresponds to $\mathrm{V_{rot}} \sin i \approx 90 \mathrm{km\,s^{-1}}$. This corresponds to a "projected radius" $\mathrm{R} \sin i \approx 0.36 R_\odot$. We have compared the colour of this star to the colour-colour diagrams of Augusteijn et al. (2008). From the $(r-i)$ v. $(i-z)$ diagram (their Fig. 2) we estimate a spectral type of ≈M1 for J1042+6442. This spectral type is consistent with the appearance of the spectrum shown in Fig. 3, e.g., the weak TiO bandhead near 4950Å is slightly stronger than the M0V star HD 79210. The mass of an M1V star is about $0.5 M_\odot$ and the radius is about $0.5 R_\odot$. Combined with the mass function $f_m = 0.093 M_\odot$, we estimate a system inclination $i \approx 45^\circ$ so the mass for the unseen companion to the M1 star $\approx 0.75 M_\odot$. There is large scatter in the relationship between mass, radius and spectral type for M-dwarfs, but these estimates are quite consistent with the companion being a white dwarf.

The radius of the Roche lobe in this system is $\approx 0.5 R_\odot$, which is comparable to the radius expected for an M1-type dwarf star. This raises the possibility that there is accretion onto the companion from the M-dwarf through the inner Lagrangian point. However, there is no evidence for an accretion disc or other accretion structures from the Hβ emission line. J1042+6442 has been detected in the ROSAT All Sky Survey (Voges 2000) with a count rate of 0.046 ± 0.011 cts/s and with a hardness ratio HR1 $= -0.29 \pm 0.20$, implying a relatively soft source. The galactic column density in the direction of J1042+6442 is $1.2 \times 10^{20} \mathrm{cm^{-2}}$ (Dickey & Lockman 1990). Given the short distance, 67 pc, we assume that about half of that column is in front of J1042+6442. Adopting a thermal Bremsstrahlung spectrum and a plasma temperature in the range $1 - 10$ keV results in an X-ray luminosity of J1042+6442 of $L_{\rm X} = (2-6) \times 10^{29}$ erg/s, which is roughly an order of magnitude lower than the typical X-ray luminosity of cataclysmic variables (Verbunt et al. 1997), but is consistent with the X-ray luminosity of rapidly rotating low-mass stars (Pizzolato et al. 2003). More specifically, adopting a 0.5 keV Raymond-Smith plasma, appropriate for coronal emission, results in $L_{\rm X} = 2 \times 10^{29}$ erg/s, which is very similar to the X-ray luminosities of the eclipsing short-period low-mass stars GU Boo, YY Gem, and CU Cnc (Ribas 2003; López-Morales & Ribas 2005). We conclude that the X-ray emission from J1042+6442 is consistent with coronal emission from the main-sequence component, corroborating the detached pre-CV nature of the system.

3.4 White dwarf effective temperatures

We have estimated the effective temperature of the white dwarfs in the three new PCEBs we have identified based on the available SDSS and GALEX photometry. We first use the SDSS $i-z$ colour of the system and the calibration of Covey et al. (2007) to estimate the spectral type of the dwarf star in these binaries. We then use the observed z-band magnitude together with the M_J and $z-J$ calibration from Covey et al. to estimate the distance to the dwarf star. J-band magnitudes are taken from the 2MASS catalogue (Skrutskie 2006). The contribution of the white

Table 3. Radial velocity and EW(Hβ) measurements for J1042+6442

MJD	V_r (km s^{-1})	$-$EW(Hβ) (Å)
54823.2846	112.0 ± 3.7	4.38 ± 0.27
54826.1419	-163.7 ± 2.9	3.78 ± 0.24
54826.2602	91.4 ± 1.8	5.48 ± 0.24
54826.2638	78.3 ± 3.0	5.52 ± 0.25
54826.2887	-64.9 ± 2.6	5.29 ± 0.26
54826.2923	-93.3 ± 2.8	4.80 ± 0.25
54826.2959	-119.4 ± 2.4	5.59 ± 0.27
54826.2995	-91.5 ± 2.9	5.50 ± 0.27
54826.3032	-117.0 ± 2.6	5.55 ± 0.29
54843.1881	26.2 ± 5.3	5.87 ± 0.67
54843.2356	142.9 ± 8.2	7.48 ± 1.0
54843.2643	45.8 ± 15.0	—
54843.2796	-57.9 ± 8.6	5.32 ± 1.1
54843.9713	15.6 ± 3.6	2.09 ± 0.36
54844.0278	184.3 ± 4.7	3.50 ± 0.21
54844.1461	-76.2 ± 3.7	3.20 ± 0.25
54844.2518	76.6 ± 5.0	4.84 ± 0.58
54844.3147	-147.1 ± 6.6	1.16 ± 0.72
54844.9890	155.1 ± 2.4	2.04 ± 0.28
54845.0185	145.3 ± 2.5	4.01 ± 0.21
54845.0760	-79.2 ± 2.8	4.84 ± 0.32
54845.1065	-166.5 ± 4.8	3.26 ± 0.20
54845.2039	172.0 ± 2.9	3.39 ± 0.20
54845.2304	118.9 ± 2.7	3.76 ± 0.20
54845.2375	77.6 ± 2.3	4.98 ± 0.22
54845.2774	-134.4 ± 4.1	3.17 ± 0.37

Table 4. Circular orbit least-squares fit to our RV measurements of J1042+6442. The model is $V_r = \gamma + K \sin[2\pi(T - T_0)/P]$ where T is the time of mid-exposure. The effect of orbital smearing due to the finite exposure time have been included. The quantity $\sigma_{\rm ex}$ is added in quadrature to the standard errors in Table 3 prior to calculating the least-squares fit and is chosen so that $\chi^2 \approx N_{\rm df}$, the number of degrees of freedom in the fit.

Parameter	Value
Period (days)	0.197669 ± 0.000022
T_0 (HJD)	2454834.7820 ± 0.0012
γ (km s^{-1})	-0.1 ± 4.4
K (km s^{-1})	166.7 ± 5.3
$\sigma_{\rm ex}$ (km s^{-1})	18
$N_{\rm df}$	22
χ^2	21.8

dwarf at these wavelengths is negligible. Synthetic spectra for the white dwarf generated using the models described in Koester et al. (2005) were then matched "by-eye" to the observed GALEX FUV and NUV fluxes by varying the effective temperature assuming the white dwarf has a surface gravity $\log g = 8.0$. The results are given in Table 5. It is difficult to make an accurate estimate of the uncertainty in these estimates. For example, the three FUV fluxes reported for J1042+6442 in GALEX GR4 are 139 ± 11, 112.2 ± 2.7 and 133.1 ± 3.9, which are clearly not consistent with a single value. We also found differences of 10 – 20 percent when we compared the distances estimated using the calibration of Covey et al. to those derived using the calibrations of Davenport et al. (2006). Changing the assumed value of $\log g$ by ± 0.5 changes the estimate of the effective temperature by about $\pm$1000K for J0941+4706 and J1042+6442, and $\pm$2000K for J1016+4935. Given these factors, our opinion is that a fair estimate of the errors in the effective temperatures of the white dwarfs is a few thousand Kelvin.

Table 5. Estimate of the white dwarf effective temperature ($T_{\rm eff,WD}$) based on the SDSS and GALEX for our three newly discovered PCEBs. The spectral type (SpTy) and distance (d) of the dwarf star based on the observed $i - z$, colours and z magnitudes are given in columns 2 and 3, respectively.

Star	SpTy	d (pc)	$T_{\rm eff,WD}$ (K)	i	$i - z$	$z - J$
J0941+4706	K7V	280	12000	14.05	0.31	1.19
J1016+4935	M2V	190	14400	13.96	0.36	1.22
J1042+6442	M3V	67	9800	12.26	0.54	1.33

4 DISCUSSION

The survey strategy we have adopted has identified one new PCEB (J1042+6442) and two stars that are also likely to be PCEBs (J0941+4706, J1016+4935) based on the amplitude and timescale of the RV variability and the narrow width of their Hβ emission lines. These new identifications are in addition to two CVs (PQ Gem and BZ UMa) and one pre-CV (BE UMa) in the sample that satisfy our selection criteria. Further observations will be required to determine the basic parameters of J0941+4706 and J1016+4935. We have compared the colours of these two stars to the colour-colour diagrams of Augusteijn et al. (2008). The dwarf star dominates the flux at these wavelengths so the colours are indistinguishable from those of single stars. The other colours of J0941+4706 are also indistinguishable from those of a single star according to the criteria of Augusteijn et al., i.e., this is a PCEB that cannot be identified from its SDSS colours alone. The colours of J1016+4935 and J1042+6442 do fall within the selection criteria of Augusteijn et al. in the $(u - g)$ v. $(g - r)$ plane (although they are near the limit), but not the $(g - r)$ v. $(r - i)$ plane. None of these stars appear in the catalogue of Augusteijn et al. because they exceed the brightness limit of $g = 16.5$ set by these authors to avoid stars with unreliable photometry. The effective temperatures we have estimated for the white dwarfs in these binaries (Section 3.4) are much lower than the temperature of the coolest WD that can be detected from a U-band excess given by Schreiber & Gänsicke (2003), which supports our conclusion that the combination of GALEX and SDSS photometry can be used to identify PCEBs that are difficult or impossible to identify using SDSS photometry alone.

Rather than setting a brightness limit, we have used the flags provided with the SDSS photometry to identify stars with reliable photometry. The brightness at which saturation of the CCD will produce unreliable photometry will depend on the filter under consideration, the colour of the

star and the seeing during the observation. It is noticeable that the SDSS photometry for several of our targets were obtained in worse-than-average seeing conditions. A full exploration of how these factors affect our survey is beyond the scope of this paper.

Two of the stars we have observed (J0754+2035 and J0851+2903) are very rapidly rotating K-dwarfs with strong chromospheric emission that show small shifts in their measured RVs. These may be the result of wind-accretion induced rapid rotation (WIRRing stars; Jeffries & Stevens 1996). The FUV-excess in these stars would then be due to the white dwarf remnant of the asymptotic giant branch (AGB) star from whose wind the K-dwarf accreted both material and angular momentum. The current separation of the WD and K-dwarf can be large in this scenario (~ 100au) so it may be possible to directly observe these WD using high resolution imaging. The apparent RV variability of these stars is likely to be dominated by spurious shifts associated with their extreme magnetic activity, i.e., star-spots, and is unlikely to be due to orbital motion. J0851+2903 can be identified as a binary star containing a WD using the criteria of Augusteijn et al. in the $(g-r)$ v. $(r-i)$ plane, but J0754+2035 would be indistinguishable from a single K-dwarf using the SDSS photometry alone.

The majority of the stars in our sample appear to be normal late-type dwarfs. There is little contamination from unidentified quasars as a result of our proper motion selection. The FUV excess in the targets that do not show radial velocity shifts in our data may be due to a hot subdwarf of hot white dwarf companion to the late-type star in wide orbit. High resolution imaging or RV measurements with greater precision than those use here could be used to confirm this hypothesis.

5 CONCLUSIONS

We have shown that complementing SDSS photometry with GALEX photometry will enable us to identify new PCEBs and WIRRing stars that cannot be identified from SDSS photometry alone. The new binary stars we have identified with our follow-up spectroscopy contain late-K or early-M dwarf stars. A more complete survey of targets identified using the methods we have developed here will be required to show whether or not the lack of PCEBs containing dwarf stars earlier than late-K is a real feature of this population.

ACKNOWLEDGMENTS

This research has made use of the SIMBAD database, operated at CDS, Strasbourg, France. PFLM would like to acknowledge discussions with R.D. Jeffries that have clarified several issues with regard to WIRRing stars. This publication makes use of data products from the Two Micron All Sky Survey, which is a joint project of the University of Massachusetts and the Infrared Processing and Analysis Center/California Institute of Technology, funded by the National Aeronautics and Space Administration and the National Science Foundation. We thank an anonymous referee for their careful reading of the manuscript.

REFERENCES

Agüeros M. A., et al. 2005, AJ, 130, 1022
Augusteijn T., Greimel R., van den Besselaar E. J. M., Groot P. J., Morales-Rueda L., 2008, A&A, 486, 843
Barcons X., Carrera F. J., Ceballos M. T., Page M. J., Bussons-Gordo J., Corral A., et al. 2007, A&A, 476, 1191
Barstow M. A., Holberg J. B., Fleming T. A., Marsh M. C., Koester D., Wonnacott D., 1994, MNRAS, 270, 499
Beer M. E., Dray L. M., King A. R., Wynn G. A., 2007, MNRAS, 375, 1000
Böehm-Vitense E., 1992, AJ, 104, 1539
Böehm-Vitense E., 1993, AJ, 106, 1113
Burleigh M., 2002, in Howell S. B., Dupuis J., Golombek D., Walter F. M., Cullison J., eds, Continuing the Challenge of EUV Astronomy: Current Analysis and Prospects for the Future Vol. 264 of Astronomical Society of the Pacific Conference Series, White Dwarfs in Sirius-Like Binaries. pp 27–+
Burleigh M. R., Barstow M. A., Fleming T. A., 1997, MNRAS, 287, 381
Covey K. R., Ivezić Ž., Schlegel D., Finkbeiner D., Padmanabhan N., Lupton R. H., Agüeros M. A., Bochanski J. J., Hawley S. L., West A. A., Seth A., Kimball A., Gogarten S. M., Claire M., Haggard D., Kaib N., Schneider D. P., Sesar B., 2007, AJ, 134, 2398
Davenport J. R. A., West A. A., Matthiesen C. K., Schmieding M., Kobelski A., 2006, PASP, 118, 1679
Davis P. J., Kolb U., Willems B., 2009, ArXiv e-prints
Dewi J. D. M., Tauris T. M., 2000, A&A, 360, 1043
Dickey J. M., Lockman F. J., 1990, ARA&A, 28, 215
Eggleton P. P., 2002, ApJ, 575, 1037
Eisenstein D. J., Liebert J., Harris H. C., Kleinman S. J., Nitta A., Silvestri N., Anderson S. A., Barentine J. C., Brewington H. J., Brinkmann J., Harvanek M., Krzesiński J., Neilsen Jr. E. H., Long D., Schneider D. P., Snedden S. A., 2006, ApJS, 167, 40
Evans P. A., Hellier C., Ramsay G., 2006, MNRAS, 369, 1229
Ferguson D. H., Liebert J., Haas S., Napiwotzki R., James T. A., 1999, ApJ, 518, 866
Han Z., Podsiadlowski P., Maxted P. F. L., Marsh T. R., Ivanova N., 2002, MNRAS, 336, 449
Heller R., Homeier D., Dreizler S., Østensen R., 2008, ArXiv e-prints
Horne K., 1986, PASP, 98, 609
Iben I. J., Livio M., 1993, PASP, 105, 1373
Jeffries R. D., Stevens I. R., 1996, MNRAS, 279, 180
Koester D., Napiwotzki R., Voss B., Homeier D., Reimers D., 2005, A&A, 439, 317
Kukarkin B. V., Kholopov P. N., Pskovsky Y. P., Efremov Y. N., Kukarkina N. P., Kurochkin N. E., Medvedeva G. I., 1971, in General Catalogue of Variable Stars, 3rd ed. (1971) The third edition containing information on 20437 variable stars discovered and designated till 1968.. pp 0–+
Landsman W., Simon T., Bergeron P., 1996, PASP, 108, 250
López-Morales M., Ribas I., 2005, ApJ, 631, 1120
Martin D. C., Fanson J., Schiminovich D., Morrissey P., Friedman P. G., Barlow T. A., et al. 2005, ApJ, 619, L1
Maxted P. F. L., Burleigh M. R., Marsh T. R., Bannister

N. P., 2002, MNRAS, 334, 833
Maxted P. F. L., Heber U., Marsh T. R., North R. C., 2001, MNRAS, 326, 1391
Maxted P. F. L., Marsh T. R., Moran C. K. J., 2002, MNRAS, 332, 745
Maxted P. F. L., Morales-Rueda L., Marsh T. R., 2004, Ap&SS, 291, 307
Mickaelian A. M., Hovhannisyan L. R., Engels D., Hagen H.-J., Voges W., 2006, A&A, 449, 425
Nelemans G., Tout C. A., 2005, MNRAS, 356, 753
Nelemans G., Verbunt F., Yungelson L. R., Portegies Zwart S. F., 2000, A&A, 360, 1011
Neustroev V. V., Zharikov S., Michel R., 2006, MNRAS, 369, 369
O'Brien M. S., Bond H. E., Sion E. M., 2001, ApJ, 563, 971
Oreiro R., Pérez Hernández F., Østensen R., Solheim J. E., MacDonald J., Ulla A., 2007, A&A, 461, 585
Paczynski B., 1976, in Eggleton P., Mitton S., Whelan J., eds, Structure and Evolution of Close Binary Systems Vol. 73 of IAU Symposium, Common Envelope Binaries. pp 75–+
Pizzolato N., Maggio A., Micela G., Sciortino S., Ventura P., 2003, A&A, 397, 147
Postnov K. A., Yungelson L. R., 2006, Living Reviews in Relativity, 9, 6
Rebassa-Mansergas A., Gänsicke B. T., Rodríguez-Gil P., Schreiber M. R., Koester D., 2007, MNRAS, 382, 1377
Ribas I., 2003, A&A, 398, 239
Rosen S. R., Mittaz J. P. D., Hakala P. J., 1993, MNRAS, 264, 171
Schreiber M. R., Gänsicke B. T., 2003, A&A, 406, 305
Schreiber M. R., Nebot Gomez-Moran A., Schwope A. D., 2007, in Napiwotzki R., Burleigh M. R., eds, 15th European Workshop on White Dwarfs Vol. 372 of Astronomical Society of the Pacific Conference Series, Understanding White Dwarf Binary Evolution with White Dwarf/Main Sequence Binaries: First Results from SEGUE. pp 459–+
Skrutskie M. F. e. a., 2006, AJ, 131, 1163
Soker N., 2004, New Astronomy, 9, 399
Soker N., Harpaz A., 2003, MNRAS, 343, 456
Stepanian J. A., 2005, Revista Mexicana de Astronomia y Astrofisica, 41, 155
Szkody P., Henden A., Mannikko L., Mukadam A., Schmidt G. D., Bochanski J. J., Agüeros M., Anderson S. F., Silvestri N. M., Dahab W. E., Oguri M., Schneider D. P., Shin M.-S., Strauss M. A., Knapp G. R., West A. A., 2007, AJ, 134, 185
Taam R. E., Sandquist E. L., 2000, ARA&A, 38, 113
Udry S., Mayor M., Queloz D., 1999, in Hearnshaw J. B., Scarfe C. D., eds, IAU Colloq. 170: Precise Stellar Radial Velocities Vol. 185 of Astronomical Society of the Pacific Conference Series, Towards a New Set of High-Precision Radial-Velocity Standard Stars. pp 367–+
Vennes S., Christian D. J., Thorstensen J. R., 1998, ApJ, 502, 763
Verbunt F., Bunk W. H., Ritter H., Pfeffermann E., 1997, A&A, 327, 602
Voges W. e. a., 2000, IAU Circ., 7432, 1
Wagner R. M., Sion E. M., Liebert J., Starrfield S. G., 1988, ApJ, 328, 213
Webbink R. F., 2008, Short-Period Binary Stars: Observations, Analyses, and Results, pp 233–+
Wegner G., Dupuis J., 1993, AJ, 106, 390
Wheatley J. M., Welsh B. Y., Siegmund O. H. W., Byun Y.-I., Yi S., Lee Y.-W., Madore B. F., et al. 2005, ApJ, 619, L123
Yanny B. e. a., 2009, AJ, 137, 4377